Title: X-band ^{1}H-DNP experiments and high power sub-THz wave irradiation effect on BDPA-doped toluene solution

M. Toda[1], Y. Fujii[1], S. Mitsudo[1], I. Ogawa[1], T. Idehara[1], T. Saito[1], H. Ito[2], M. Chiba[2]

[1]Research Center for Development of Far-Infrared Region, University of Fukui,
3-9-1 Bunkyo, Fukui 910-8507, Japan

[2]Department of Applied Physics, University of Fukui,
3-9-1 Bunkyo, Fukui 910-8507, Japan

A short title: DNP-experiments on BDPA-doped Toluene Solution

Dr. Mitsuru Toda,
[1]Research Center for Development of Far-Infrared Region, University of Fukui,
3-9-1 Bunkyo, Fukui 910-8507, Japan
E-mail : toda@fir.fukui-u.ac.jp

I. ABSTRACT

To investigate the experimental technique and the high magnetic field effect in the dynamical nuclear polarization (DNP) experiments, the X-band ^{1}H-DNP and the high power sub-THz wave irradiation experiments have been performed on bis-diphenylene-phenyl-allyl (BDPA)-doped toluene solution at room temperature. We have established the sample-shuttle X-band DNP experimental system, and investigated the external magnetic field, the microwave power and ^{1}H-T_1^{-1} dependences of Overhauser enhancement factor (ε). A maximal signal enhancement of approximately –19 has been observed. As for the sub-THz wave experiments, we have constructed the NMR and ESR measurement system for the experiments under the magnetic field of ~10.7 T, with a high power light source gyrotron CW-I ($TE_{22,8}$ mode, f~299.23 GHz). When the high power sub-THz wave of a gyrotron was irradiated on the toluene solution in order to confirm the evidence of DNP, the sample has evaporated due to the electromagnetic (EM) wave heating.

II. INTRODUCTION

DNP is one variation of double resonance technique in NMR spectroscopy, which has history of more than 50 years. Recently, there were some events and many NMR and ESR researchers have come to think that DNP is a promising method in near future in the research field of NMR. One event is the appearance of the commercial product “hypersense” by Oxford instruments. Another trend has arisen from the consecutive research activities by Griffin and his coworker’s at MIT [1-24]. They have pushed up the high magnetic field limit of DNP experiments with a “gyrotron”, which operates at 140 GHz and 250 GHz, corresponding to the ESR field of 5 T and 9 T. So far, a gyrotron is the only watt class high power light source in the power gap region of millimeter and submillimeter waves, which has been used for the DNP and ESR experiments [1-30]. A free electron laser is a high power light source in the same frequency region, however, it is not familiar to the magnetic resonance experiment yet.

The main research activity at our center (Research Center for Development of Far-Infrared Region; FIR) is to develop an original gyrotron and explore its application (ESR, DNP, etc). The research of DNP-NMR has started at FIR from about 2 years ago. The purpose is to build up the high magnetic field DNP technique to apply for the protein structural analysis, and to find other applicable systems. However, if we directly begin the submillimeter wave DNP experiments at very low temperature without experience of DNP experiments at lower fields, many difficulties might appear; such as the consumption of liquid helium and electric power at 2 superconducting magnets (SCMs) plus sample cooling system.

In this paper we report the first stage of development of DNP-NMR at FIR. We have developed the sample-shuttle X-band DNP experimental system with an Yttrium-iron-garnet (YIG) oscillator

and a traveling wave tube amplifier (TWTA) as a microwave source. And for the sub-THz wave experiments, we have constructed the NMR and ESR measurement system for the experiments under the magnetic field of ~10.7 T, with a high power light source gyrotron CW-I ($TE_{22,8}$ mode, f~299.23 GHz). To confirm the performance of the newly developed system, we have looked for the already known and easily available sample in which DNP has been observed at room temperature [31]. Through the experiments on BDPA-doped toluene solution with these two experimental systems, we have started our first approach to the high magnetic field DNP experiment.

III. MATERIAL AND METHODS

DNP experiments have been usually performed at low temperatures, because the required microwave power is typically below ~100mW at liquid He temperature (this power level is even achievable by a Gunn oscillator). On the other hand, DNP has been observed at higher temperatures (room temperature) in many samples, and the former DNP experiment on BDPA-doped toluene solution seems to be a good example for us to follow from the following reasons. It is easy to obtain the materials (BDPA from Sigma-Aldrich), the materials contain protons, and ^{1}H-T_1 is rather long at the order of a few seconds, which is convenient for the sample-shuttle system.

Schematic diagram of the X-band DNP system is shown in Fig. 1. The system is composed of a

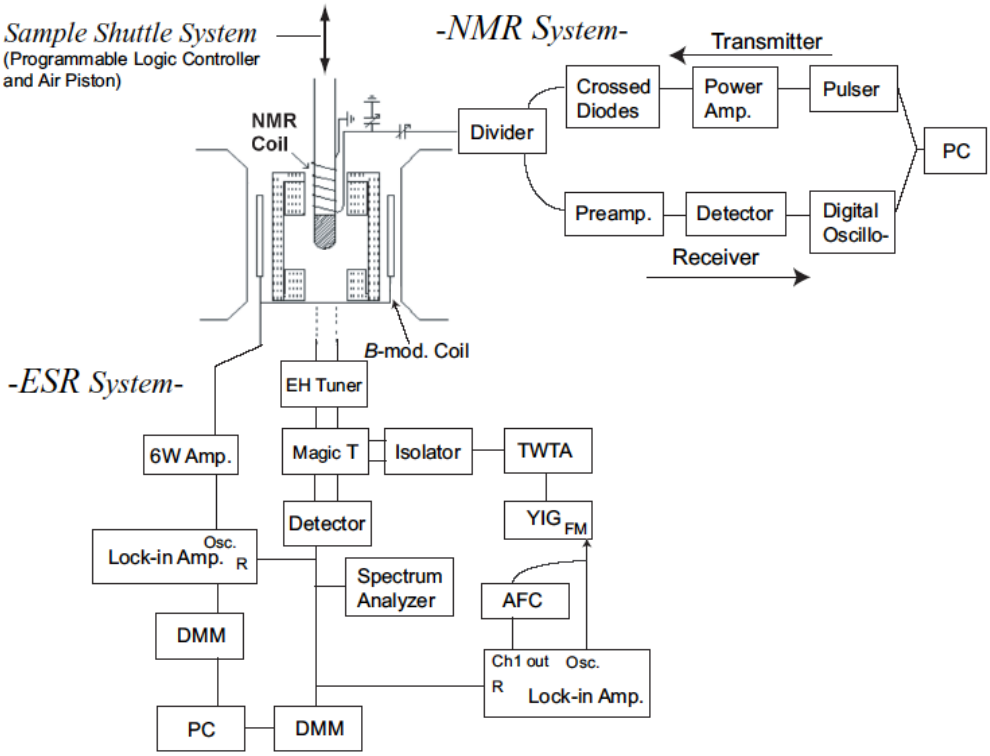

Fig. 1

conventional 5-to-220MHz 300W NMR instrument (which is usually used for the research of solid-state physics), the X-band ESR measurement system with a TE_{011} cylindrical cavity, the sample shuttle system, and a 2 T electromagnet with pole pieces.

As for the microwave source of ESR, we have used a YIG oscillator and a TWTA. The output from a TWTA is in the frequency range of 8~12.4 GHz, and the maximum power is more than ~15 W. For the ESR measurement and enhancement of the magnetic field at the sample, a frequency tunable TE_{011} mode cylindrical cavity (11.2~11.6 GHz, Q~2x10^4) has been fabricated [32]. The microwave frequency of a YIG oscillator was externally regulated by a lock in amplifier and the feedback circuit, and the frequency is stabilized to the cavity resonant frequency at the precision of ~0.1 MHz. A Cu-coil is positioned beside the cavity to yield the *B*-field modulation at the sample position, and intensity of the reflected microwave is measured at a lock-in amplifier and a digital multi-meter. To avoid interference, the NMR-coil is positioned outside and adjacent to the cavity resonant space. The "sample shuttle system" is made with a PLC (Programmable Logic Controller) and an air-piston. The sample is put in a glass tube, and transport between the NMR-coil and the resonant cavity center within ~0.1 s.

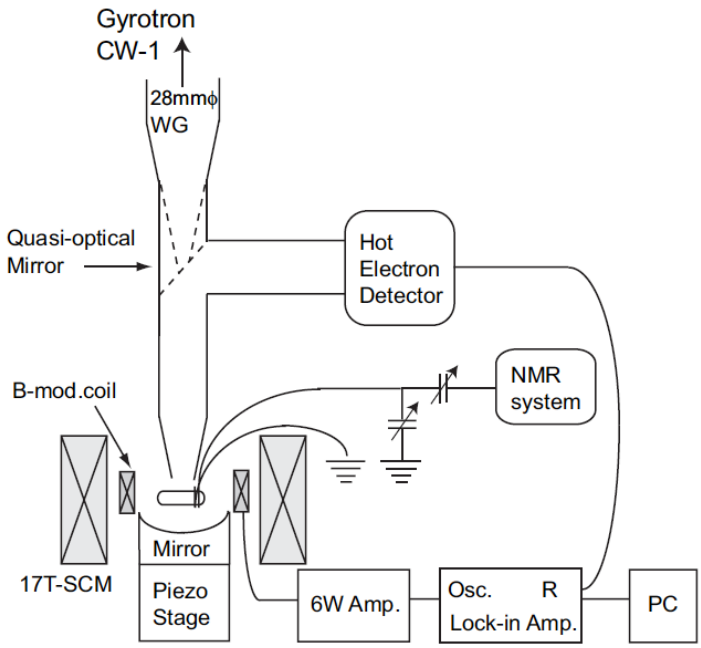

Fig. 2

Figure 2 shows schematic diagram of the sub-THz wave ESR and NMR experimental system. A

gyrotron CW-I has been used for the ESR light source, which is developed at FIR. A gyrotron CW-I operates at $TE_{22,8}$ mode (f~299.23 GHz) and the output power at the window is more than ~1.7 kW. The high power sub-THz wave is transmitted by the ϕ28 waveguide to the top of 17T-SCM, and the power is >150 W there. The waveguide is tapered, and ϕ4 waveguide end constitutes the cavity with the reflecting mirror. The sub-THz wave power has not been measured at the sample position. The cavity length has been adjusted by a piezo z-stage.

The sample shuttle system is not used for the sub-THz wave system. The NMR coil is wound around the sample glass tube, and shifted slightly from the sub-THz wave irradiation position, in order to minimize the interference. The reflected sub-THz wave is measured at the hot electron detector. The power fluctuation of a gyrotron is more than 1% owing to the noise of the power source of the cathode voltage. The magnetic field modulation method was applied and a lock-in amplifier is used to detect the ESR signal in the magnetic B-field sweep measurement.

IV. RESULTS

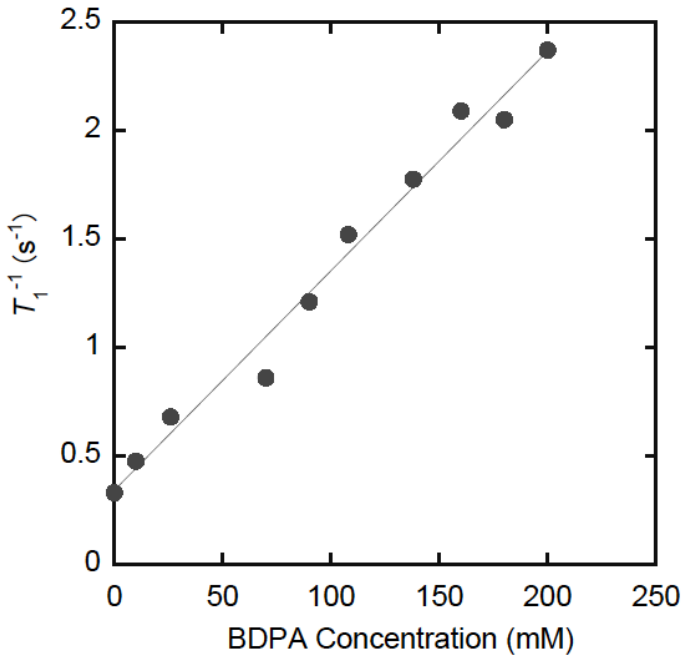

Fig. 3

Figure 3 shows the experimental results for the relaxation rate of proton in toluene solution as a function of the radical concentration. The experiments have been carried out under B=0.4 T, at the NMR frequency of 17.3 MHz, and at room temperature. Without radical, the nuclear spin relaxation

time T_1 of proton in toluene liquid is ~3 s. When the BDPA radical is doped, the relaxation rate T_1^{-1} has shown the tendency to increase linearly [34]. The significant hyperfine interaction between the BDPA radical spin and ^{1}H of toluene can be confirmed.

We first describe the X-band DNP experimental results. Figure 4 shows the microwave power dependence of the ^{1}H-NMR spin echo signal. ESR frequency is ~11.31 GHz (ESR frequency is fixed at ~ 11.31 GHz in this paper), NMR frequency ~17.3 MHz, and ^{1}H-T_1^{-1}~1.47 s^{-1}. As the microwave power is increased, the intensity of spin echo signal first decreases, and then largely increased to the negative direction. The effect of microwave irradiation seems to saturate at ~10 W. The results

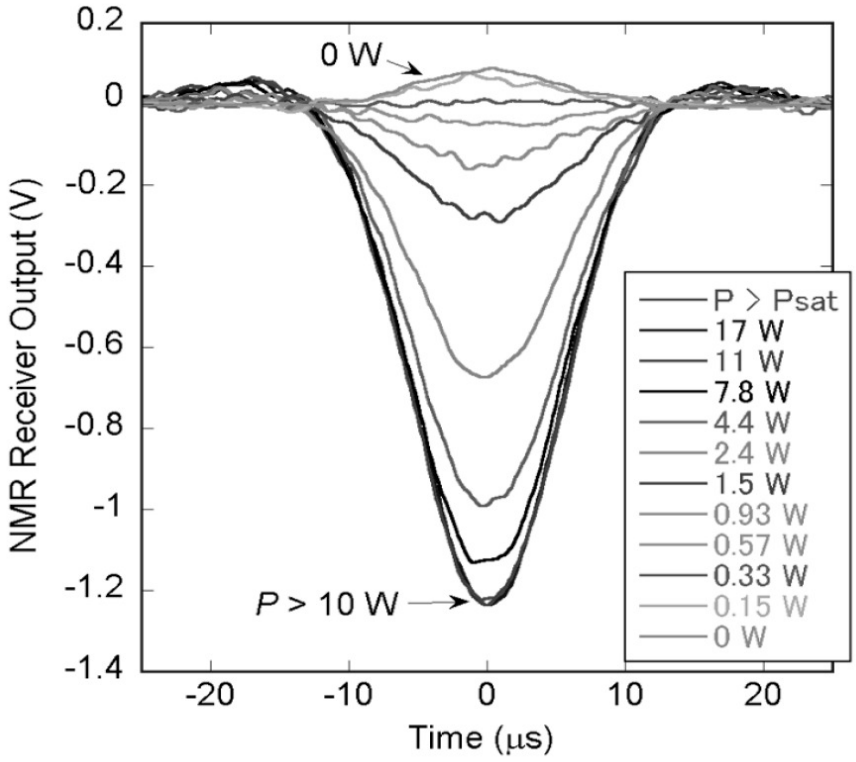

Fig. 4

indicate the existence of the Overhauser effect of the dipolar interaction origin.

Here we define the Overhauser enhancement factor as $\varepsilon = \langle I_z \rangle / \langle I_0 \rangle$, where $\langle I_z \rangle$ is the nuclear polarization rate when the microwave is irradiated and $\langle I_0 \rangle$ is the nuclear polarization rate without the microwave. In Fig. 5, we show the result of ESR measurement for the BDPA crystal (not in toluene solution) and the data of Overhauser enhancement factor ε as a function of the external magnetic field. $|\varepsilon|$ is largest at the ESR field. From the results shown in Fig. 4 and 5, we can confirm the magnetic field and the microwave power dependences, characteristic to the Overhauser effect.

S/N ratio of the ESR data is not good in Fig. 5. This is mainly due to the fact that the modulation

magnetic field is weak. We could not wound the thick Cu coil to the cavity, because of the small distance between the pole pieces of a 2T electromagnet. For the same reason, we could not measure the solution ESR data, thus the ESR data of the solid crystal sample is shown in Fig. 5.

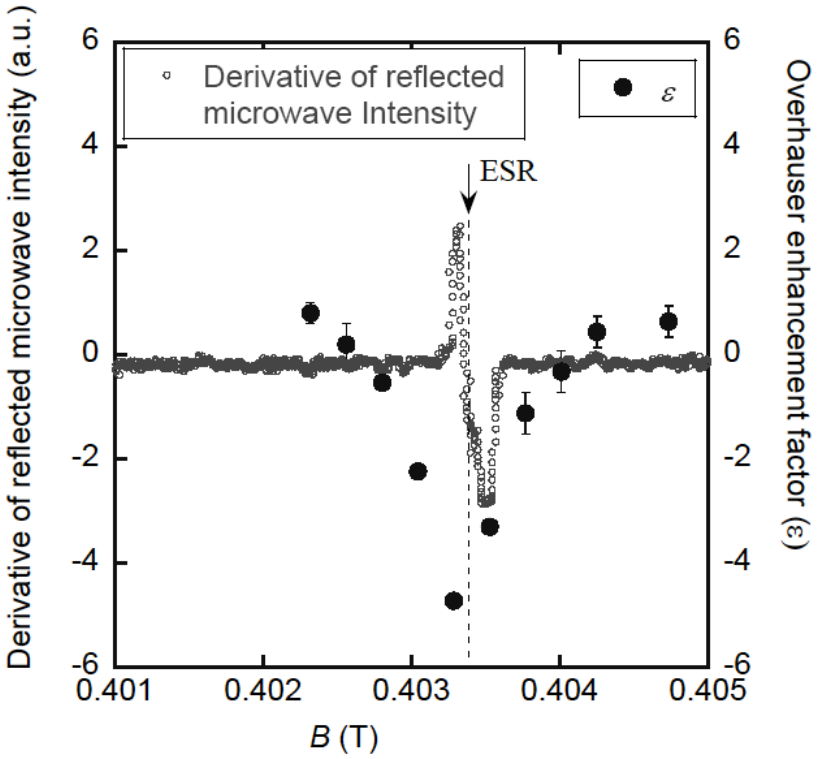

Fig. 5

For the sub-THz wave experiments, we have used ^{13}C-enriched toluene (C_6H_5-$^{13}CH_3$), because we could not measure proton signal under such high magnetic field with our NMR instrument (5~220MHz). The ESR signal of BPDA radical and the ^{13}C-NMR signal from ^{13}C enriched toluene (C_6H_6-$^{13}CH_3$) have been observed respectively. But when the power of the sub-THz wave is increased, the sample temperature has rapidly increased, and toluene solution has evaporated. Under the power limit where the evaporation is not too severe, there was no evidence of DNP for ^{13}C-NMR signal induced by the sub-THz wave irradiation. For the toluene solution sample, the setting shown in Fig. 2 is insufficient to confirm the DNP effect.

V. DISCUSSION

For the analysis, we refer to the method described in ref. 33 and 34. Overhauser enhancement factor ε is given by

$$1-\varepsilon = \rho\, f\, s\, \gamma_e / \gamma_n. \quad (1)$$

In Eq. (1), ρ is the coupling factor, f is the leakage factor, s is the saturation factor, γ_e and γ_n are the gyromagnetic ratio of electron and proton, respectively. The saturation factor s depends on the power of the irradiation microwave P, and it can be approximated as

$$s=\gamma_e^2 B_1^2 T_{1e} T_{2e}/(1+\gamma_e^2 B_1^2 T_{1e} T_{2e})=\beta P/(1+\beta P), \quad (2)$$

where B_1 is the amplitude of the oscillating B-field, T_{1e} and T_{2e} are the spin-lattice relaxation time and the spin-spin relaxation time of electron, respectively, and we have put $T_{1e}T_{2e}\gamma_e^2 B_1^2 = \beta P$.

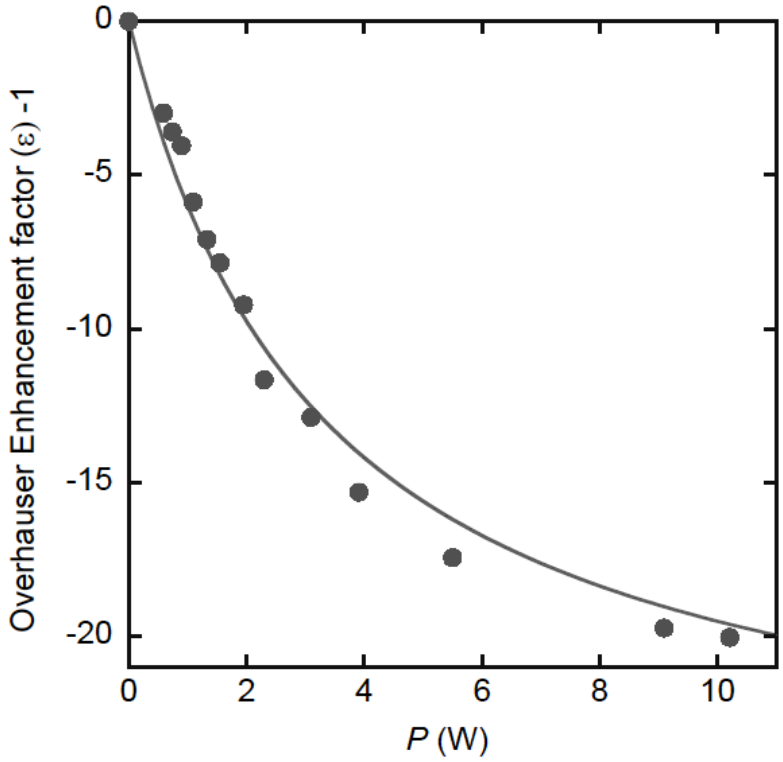

Fig. 6

Figure 6 shows the experimental results for Overhauser enhancement factor ε plotted as a function of the microwave power, and fit to Eq. (2). NMR frequency is ~16.98 MHz, and ^{1}H-T_1^{-1}~1.6 s^{-1}. The fitted curve is obtained with β~0.3. Substituting the values of ε=–19, s=0.75,

and f=0.8, ρ is estimated as –0.051 for this sample.

The leakage factor f depends on the relaxation rate of ^{1}H, and is given by

$$f=R_{II}/(R_0+R_{II}). \quad (3)$$

R_{II} is the ^{1}H relaxation rate induced by BDPA radical, and R_0 is the ^{1}H relaxation rate induced by the molecular motion of toluene. Figure 7 shows the observed values of ε as a function of ^{1}H-T_1^{-1} for P~10 W. ^{1}H-T_1^{-1} are varied by adding the BDPA crystal into the sample and changing the radical concentration. The dash-dotted curve is fit to Eq. (3).

The value of ε is ~−19 for T_1^{-1}~1.6 and P~10 W in Fig. 6. On the other hand, in Fig. 7, the value of ε is ~−11 for T_1^{-1}~1.5. The BDPA concentrations and the microwave irradiation power are approximately the same between these two experiments, but the observed values of ε are different. We have not degassed the toluene solution, and this fact may be the reason. The sample has been usually damaged within 1~2 days, and then did not show DNP effect. The data in Fig. 7 have been measured in 10 hours to minimize the effect from the change of the sample quality.

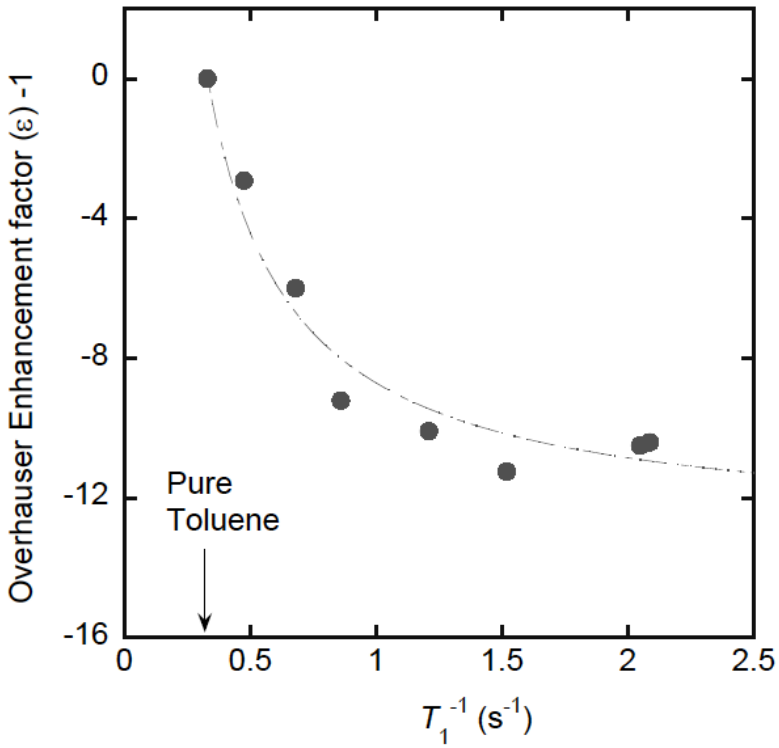

Fig. 7

When the results of DNP at 11 GHz and 40 GHz [31] are compared, $|\varepsilon|$ is larger at 40 GHz (ε~−40). If we only consider translational motion of toluene, then this is unnatural [23, 35, 36]. It is known that BDPA frequently produce strong contact of relatively long duration with solvent molecules. In such case, the frequency dependence of ρ becomes complicated because of the scalar

coupling between the electron and nuclear spin [23, 36]. However, the phenomenon is significant for ^{19}F and ^{31}P, and rather weak for proton DNP. Thus for our case, we regard that the main reason can be attributed to the fact that we have not degassed the sample.

According to the results of high power sub-THz wave irradiation experiments, we have to pay more efforts to depress the effect of electric field. It is widely recognized that the dielectric constant is very small for toluene. However, there is an internal rotation of metyl-group at ~600 GHz and at lower frequencies [37], so some molecular motion of toluene may have the same frequency of the irradiated EM wave.

At first, we have thought one way to avoid increase of the sample temperature is to minimize the sub-THz wave irradiation time. Figure 8 shows the X-band ^{1}H-DNP experimental results for ε as a function of the microwave irradiation time. The microwave power is ~2 W, and NMR frequency ~17.33 MHz. The sample shuttle system has been effectively used to change the microwave irradiation time. As shown, the irradiation time of more than ~5 s is needed for saturation. The fitted curve is obtained by assuming the exponential time variation of the DNP ratio. The time constant for the DNP build-up rate is τ_{DNP}~1.78 s in Fig. 8, which is approximately the same with the proton relaxation time (T_1~1.47 s). If more than three times T_1 time is needed for full DNP build-up, we need ~10 s for the case of ^{13}C at 10.7 T (^{13}C-T_1~3 s). This is too long compared with the temperature increase rate of the toluene solution.

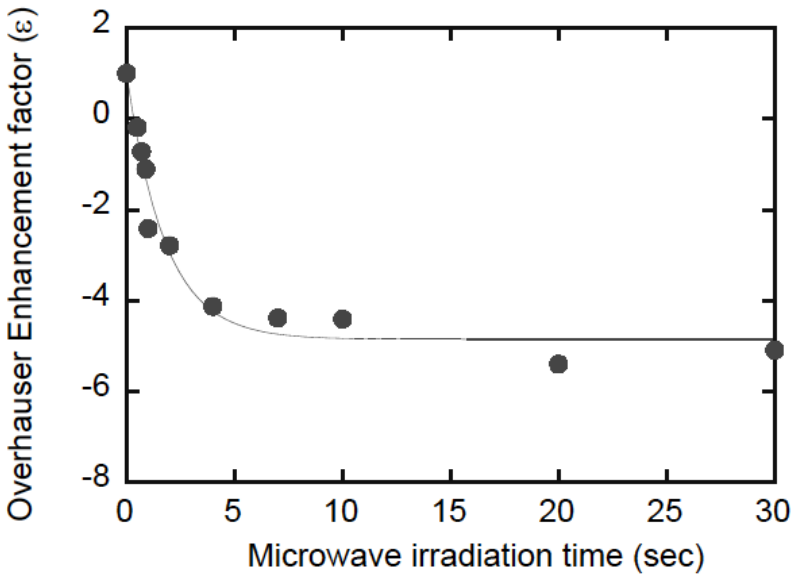

Fig. 8

The feasible solution is to perform the experiments at the cryogenic temperature. Development of the sub-THz wave DNP system with such an improvement is our current subject.

VI. ACKNOWLEDGEMENTS

The authors are very grateful to Dr. K. Takeda at Kyoto University, Japan, for kind suggestions and discussions with regard to the "sample shuttle system".

REFERENCES

[1] Becerra L. R., Gerfen G. J., Temkin R. J., Singel D. J., and Griffin R. G.: Phys. Rev. Lett. **22**, 3561 (1993)

[2] Gerfen G. J., Becerra L. R., Hall D. A., Singel D. J., and Griffin R. G.: Jour. Chem. Phys. **102** (24), 9494-9497 (1995)

[3] Hall D. A., Maus D. C., Gerfen G. J., Inati S., Becerra L. R., Dahlquist F.W., and Griffin R. G.: Science **276**, 930-931 (1997)

[4] Weis V., Bennati M., Rosay M., Bryant J. A., and Griffin R. G.: J. Magn. Res. **140**, 293-299 (1999)

[5] Farrar C. T., Hall D. A., Gerfen G. J., Rosay M., Ardenjaer-Larsen J. -H., and Griffin R. G.: J. Magn. Res. **144,** 134-141 (2000)

[6] Farrar C. T., Hall D. A., Gerfen G. J., Inati S. J. and Griffin R.G.: J. Chem. Phys. **114**, 4922-4933 (2001)

[7] Rosay M., Zeri A., Astrof N. S., Opella S. J., Herzfeld J., and Griffin R. G.: J. Am. Chem. Soc. **123,** 1010-1011 (2001)

[8] Bajaj V. S., Farrar C. T., Hornstein M. K., Mastovsky I., Bryant J., Kreischer K. E., Elena B., Vieregg J., Temkin R. J., and Griffin R. G.: J. Magn. Resonance **160**, 85-90 (2003)

[9] Rosay M., Lansing J., Haddad K. C., Bachovchin W. W., Herzfeld J., Temkin R. J., and Griffin R. G.: J. Amer. Chem. Soc. **125**, 13626-27 (2003)

[10] Hu K. -N., Yu H. -h., Swager T. M., Griffin R. G.: J. Am. Chem. Soc. **126**, 10844-10845 (2004)

[11] Song C., Hu K. -N., Swager T. M., Griffin R. G.: J. Am. Chem Soc. **128**, 11385-11390 (2006)

[12] P. C. A. van der Wel, Hu K. -N., Lewandowski J., Griffin R.G.: J. Am. Chem. Soc. **128**, 10840-10846 (2006)

[13] Hu K. -N., Bajaj V. S., Rosay M. and Griffin R.G.: J. Chem. Phys. **126**, 044512 (2007)

[14] Mak M. L., Bajaj V. S., Hornstein M. K., Belenky M., Griffin R. G., and Herzfeld J.: Proc. Nat' l. Acad. Sci. **105**, 883-888 (2008)

[15] Becerra L. R., Gerfen G. J., Bellew B. F., Bryant J. A., Hall D. A., Inati S. J., Weber R. T., Un

S., Prisner T. F., McDermott A. E., Fishbein K. W., Kreischer K. E., Temkin R. J., Singel D. J., and Griffin R. G.: Jour. Magn. Reson. A **11**7, 28-40 (1995)

[16] Hornstein M. K., Bajaj V. S., Griffin R. G., Kreischer K. E., Mastovsky I., Shapiro M. A., Sirigiri J. R., and Temkin R. J.: IEEE Transactions on Electron Devices **52**, 798-807 (2005)

[17] Woskov P. W., Bajaj V. S., Hornstein M. K., Temkin R. J., and Griffin R. G.: IEEE Transactions on Microwave Theory and Techniques **53,** 1863-1869 (2005)

[18] Joye C. D., Griffin R. G., Hornstein M. K., Hu K.-N., Kreischer K. E., Rosay M., Shapiro M. A., Sirigiri J. R., Temkin R. J., and Woskov P. P.: IEEE Transactions on Plasma Science **34**, 518-523 (2006)

[19] Bajaj V. S., Hornstein M. K., Kreischer K. E., Woskov P. P., Sirigiri J. R., Woskov P. P., Mak M. L., Herzfeld J., Temkin R. J., and Griffin R.G.: Jour. Magn. Reson. **189,** 251-279 (2007)

[20] Un S., Prisner T., Weber R.T., Seaman M. J., Fishbein K. W., McDermott A. E., Singel D. J., and Griffin R. G.: Chem. Phys. Lett. **189**, 54 (1992)

[21] Weis V., Bennati M., Rosay M., and Griffin R.G.: J. Chem. Phys. **113,** 6759-6802 (2000)

[22] Weis V., and Griffin R.G.: Solid State Nuclear Magnetic Resonance **29**, 105-117 (2006)

[23] Loening N. M., Rosay M., Weis V., and Griffin R. G.: J. Am. Chem. Soc. **124,** 8808-8809 (2002)

[24] Joo C. -G., Hu K. -N., Bryant J. A., and Griffin R. G.: J. Am. Chem. Soc. **128**, 9428-9432 (2006)

[25] Tatsukawa, T., Maeda T., Sasai H., Idehara T., Mekata M., Saito T., and Kanemaki T.: Int. J. Infrared and Millimeter Waves, **16**, 293-305 (1995)

[26] Aripin, Mitsudo S., Shirai T., Matsuda K., Kanemaki T., Idehara T., and Tatsukawa T.: Int. J. Infrared and Millimeter Waves, **20**, 1875-1888 (1999)

[27] Chiba M., Aripin, Kitai K., Mitsudo S., Idehara T., Ueda S., Toda M.: Physica B, Condensed Matter **294-295**, 64-67 (2001)

[28] Chiba M., Kitai K., Mitsudo S., Idehara T., Ueda S., and Toda M. in: Gyrotron ESR in $CsFeCl_3$ up to 40 T (Kawamori A., Yamauchi J., Ohta H., eds.), pp. 779-783, EPR in the 21st Century: Basics and Applications to Material, Life and Earth Sciences: Proceedings of the Third Asia Pacific EPR/ESR Symposium Kobe, Elsevier, 2001.

[29] Chiba M., Higuchi T., Kitai K., Mitsudo S., Idehara T., Toda M., and Ueda S.: Physica B, Condensed Matter **329-333**, 950-951 (2003)

[30] Mitsudo S., Higuchi T., Kitai K., Kanazawa K., Idehara T., Ogawa I., and Chiba M.: J. Phys. Soc. Jpn. **72**, Suppl. B, 172-176 (2003)

[31] Wind R. A., Ardenkjær-Larsen J. H., Hu J. Z., Bai S., Solum M. S., Grant D. M., Pugmire R. J., Ellis P. D., and Yonker C. R.: Macromolecular Structure and Dynamics 1999 Annual Report 2-21.

[32] C. P. Poole, Jr.: Electron Spin Resonance: A Comprehensive Treatise on Experimental Techniques, 2nd Edition, p. 142, US, Dover, 1997.

[33] Wind R. A. and Ardenkjær-Larsen J. H.: J. Magn. Reson. **141**, 347-354 (1999)

[34] Ardenkjær-Larsen J. H., Laursen I., Leunbach I., Ehnholm G., Wistrand L.-G., Petersson J. S., and Golman K.: Journal of Magnetic Resonance **133**, 1-12 (1998)

[35] G. J. Krüger, W. Müller-Warmuth, and R. Van Steenwinkel: Z. Naturforsch. **21a**, 1224-1230 (1966)

[36] W. Müller-Warmuth and K. Meise-Gresch: Advances in Magnetic Resonance (J. S. Waugh, Ed.), Vol. 11, 1-45 (1983)

[37] Murakami J., Ito M., and Kaya K.: Chem. Phys. Letters **80**, 203-206 (1981)

Fig. 1 Schematic diagram of the X-band DNP experimental system. The system is composed of a conventional 5-to-220MHz 300W NMR instrument, an X-band ESR measurement system with a TE_{011} cylindrical cavity, the sample shuttle system, and a 2T electromagnet.

Fig. 2 Schematic diagram of the sub-THz wave ESR and NMR experimental system. A gyrotron CW-I is used as a light source, which is developed at FIR research center. The waveguide is tapered, and ϕ4 waveguide end constitutes the cavity with the reflecting mirror. The NMR coil is wound around the sample glass tube, and shifted slightly from the sub-THz wave irradiation position.

Fig. 3 The relaxation rate of proton in toluene solution has shown the tendency to increase linearly as a function of the radical concentration. The experiments have been carried out under B=0.4 T, at the NMR frequency of 17.3 MHz.

Fig. 4 The microwave power dependence of the ^{1}H-NMR spin echo signal. ESR frequency is ~11.31 GHz (ESR frequency is fixed in this paper), NMR frequency ~17.3 MHz, and ^{1}H-T_1^{-1}~1.47 s^{-1}. As the microwave power is increased, the intensity of spin echo signal first decreases, and then largely increased to the negative direction. The effect of microwave irradiation seems to saturate at ~10 W. The results indicate the existence of the Overhauser effect of the dipolar interaction origin.

Fig. 5 The ESR signal of BDPA crystal and the data of Overhauser enhancement factor ε plotted as a function of the external magnetic field. NMR frequency has been changed with resonant B-field between 16.98~17.09 MHz. We can see that $|\varepsilon|$ is largest at the ESR field.

Fig. 6 The experimental results for Overhauser enhancement factor ε plotted as a function of the microwave power, and fit to Eq. (2). NMR frequency is ~16.98 MHz, and ^{1}H-T_1^{-1}~1.6 s^{-1}. The fitted curve is obtained with β ~0.3.

Fig. 7 The observed values of ε are plotted as a function of the proton relaxation rate. The microwave power is ~10 W, and NMR frequency ~17.33 MHz. The correspondence between the BDPA concentration and the proton relaxation rate has been already shown in Fig. 3. The dash-dotted curve is fit to Eq. (3), which approximately explains the observed behavior.

Fig. 8 The X-band ^{1}H-DNP experimental results for ε as a function of the microwave irradiation time. The microwave power is ~2W, NMR frequency ~17.33MHz, ^{1}H-T_1^{-1}~1.6 s^{-1}. The fitted curve is obtained by assuming the exponential time variation of the DNP build-up ratio. The time constant of DNP build-up rate, τ_{DNP}~1.78s, is approximately the same with the proton relaxation time (T_1~1.47s).